
This is an electronic reprint of the original article.
This reprint may differ from the original in pagination and typographic detail.

Sahivirta, Hanna; Wilson, Benjamin P.; Lundström, Mari; Serna-Guerrero, Rodrigo

A study on recovery strategies of graphite from mixed lithium-ion battery chemistries using froth flotation

Published in:
Waste Management

DOI:
[10.1016/j.wasman.2024.03.032](https://doi.org/10.1016/j.wasman.2024.03.032)

Published: 15/05/2024

Document Version
Publisher's PDF, also known as Version of record

Published under the following license:
CC BY

Please cite the original version:
Sahivirta, H., Wilson, B. P., Lundström, M., & Serna-Guerrero, R. (2024). A study on recovery strategies of graphite from mixed lithium-ion battery chemistries using froth flotation. *Waste Management*, 180, 96-105. <https://doi.org/10.1016/j.wasman.2024.03.032>

This material is protected by copyright and other intellectual property rights, and duplication or sale of all or part of any of the repository collections is not permitted, except that material may be duplicated by you for your research use or educational purposes in electronic or print form. You must obtain permission for any other use. Electronic or print copies may not be offered, whether for sale or otherwise to anyone who is not an authorised user.



Research Paper

A study on recovery strategies of graphite from mixed lithium-ion battery chemistries using froth flotation

Hanna Sahivirta, Benjamin P. Wilson, Mari Lundström, Rodrigo Serna-Guerrero*

Department of Chemical and Metallurgical Engineering (CMET), School of Chemical Engineering, Aalto University, Vuorimiehentie 2, 02150, Espoo, Finland



ARTICLE INFO

Keywords:

Battery Recycling
Direct recycling
Graphite
LTO
NMC811
Froth flotation

ABSTRACT

The growing electric vehicle industry has increased the demand for raw materials used in lithium-ion batteries (LIBs), raising concerns about material availability. Froth flotation has gained attention as a LIB recycling method, allowing the recovery of low value materials while preserving the chemical integrity of electrode materials. Furthermore, as new battery chemistries such as lithium titanate (LTO) are introduced into the market, strategies to treat mixed battery streams are needed. In this work, laboratory-scale flotation separation experiments were conducted on two model black mass samples: i) a mixture containing a single cathode (i.e., NMC811) and two anode species (i.e., LTO and graphite), simulating a mixed feedstock prior to hydrometallurgical treatment; and ii) a graphite-TiO₂ mixture to reflect the expected products after leaching. The results indicate that graphite can be recovered with > 98 % grade from NMC811-LTO-graphite mixtures. Additionally, it was found that flotation kinetics are dependent on the electrode particle species present in the suspension. In contrast, the flotation of graphite from TiO₂ resulted in a low grade product (<96 %) attributed to the significant entrainment of ultrafine TiO₂ particles. These results suggest that flotation of graphite should be preferably carried out before hydrometallurgical treatment of black mass.

1. Introduction

Lithium-ion batteries (LIBs) have gained popularity in the electric vehicle (EV) industry due to their high energy, power densities and long cycle lives. Compared to internal combustion engine (ICE) vehicles, it has been widely claimed that EVs have the potential to significantly reduce the transportation sector's greenhouse gas emissions, making e-mobility a non-trivial factor in the mitigation of global anthropogenic climate change (Gaines et al., 2019). On the other hand, the rapid increase in EVs production also raises concerns about raw material availability and the associated environmental impact of the LIBs life cycle. For instance, according to the EU battery regulatory framework, 70 % of the LIB materials need to be recovered from 2030 onwards to satisfy the increasing raw material demands for future LIB production and to reduce the need of virgin raw materials (European Commission, 2020).

The most common cathode active materials used in LIBs are lithium metal oxides and phosphates such as LiCoO₂ (LCO), LiFePO₄ (LFP), LiMn₂O₄ (LMO), LiNi_{1/3}Mn_{1/3}Co_{1/3}O₂ (NMC111) and LiNiCoAlO₂

(NCA) (Costa et al., 2021, Doose et al., 2021, Kim et al., 2021). NMC is a popular cathode material in EV applications as Co and Ni provide high energy density structures while the Li and Mn oxide forms a spinel structure which improves the thermal stability of the cathode (Changes et al., 2015, Wang et al., 2019). Recent developments of NMC cathodes are moving towards high nickel and low cobalt and manganese compositions such as LiNi_{0.8}Mn_{0.1}Co_{0.1}O₂ (NMC811) due to cost savings, supply risk, and ethical concerns of Co production, as well as increasing energy density requirements (Changes et al., 2015, Jena et al., 2021).

Currently, most commercial anodes in LIBs consist of graphite, which is a non-toxic, material with high specific capacity, relatively good mechanical strength, thermal and chemical stability. Nevertheless, the volumetric changes in the graphite due to Li⁺ intercalation form cracks exposing fresh graphite that readily reacts with the organic electrolyte inducing solid electrolyte interface (SEI) formation, which decreases the availability of ions and results in battery failure (Paligaro et al., 2019, Wang et al., 2019).

As an alternative to graphite, spinel structured lithium titanium oxide Li₄Ti₅O₁₂ (LTO) anodes have entered the EV markets due to their

* Corresponding author.

E-mail addresses: hanna.sahivirta@aalto.fi (H. Sahivirta), ben.wilson@aalto.fi (B.P. Wilson), mari.lundstrom@aalto.fi (M. Lundström), rodrigo.serna@aalto.fi (R. Serna-Guerrero).

<https://doi.org/10.1016/j.wasman.2024.03.032>

Received 8 December 2023; Received in revised form 5 March 2024; Accepted 27 March 2024

Available online 1 April 2024

0956-053X/© 2024 The Authors. Published by Elsevier Ltd. This is an open access article under the CC BY license (<http://creativecommons.org/licenses/by/4.0/>).

good structural stability and fast charging capabilities (Casals et al., 2017). Presently, companies like Altairnano and Toshiba are the leading LTO battery cell manufacturers and EV manufacturers such as Lightning Car Company (Page, 2008), Phoenix Motorcars (Kane, 2020), and Proterra (Proterra, 2024) have implemented Altairnano LTO batteries to their electric vehicles. The LTO battery launched by Toshiba commercially known as Super Charge Ion Battery (SCiB) is reportedly used to power Mitsubishi iMiEV Japan limited version and Minicab MiEV (Integrity exports, 2019) and JR Central N700S Shinkansen high speed electric train uses Toshiba's LIB cells (Kingsley, 2019). It is thus expected that LTO batteries will soon be found in the battery waste streams at their end-of-life (EoL).

The current state-of-the-art industrial scale LIB recycling facilities primarily focus on recovering the most expensive metals such as Co, Ni and Cu while neither graphite nor Li are recovered due to their perceived low economic value (Chernyaev et al., 2023, Costa et al., 2021, Jena et al., 2021, Salces et al., 2022, Vanderbruggen et al., 2021a, Velazquez-Martinez et al., 2019). However, graphite represents 14–22 % of a LIBs weight and therefore, it should be recovered to satisfy the expected EU recycling requirements (Chernyaev et al., 2023, Vanderbruggen et al., 2021a, Vanderbruggen et al., 2022b). In addition, the EU considers Ni and Cu as strategic raw materials while Co, Li, Mn, Ti, natural graphite, and bauxite are categorized as critical raw materials (European Commission, 2023) highlighting the importance of developing viable recycling strategies for these elements.

To recover broader range of elements from spent LIBs, the focus has shifted towards hydrometallurgical recycling options (Or et al., 2020, Salces et al., 2022). The metallic elements from the waste LIB electrodes are typically leached in acidic media with a reducing agent (typically H_2SO_4 with H_2O_2), which produces a pregnant leach solution (PLS). Recent efforts have also shown that Ni, Mn, Co and Li can be recovered from NMC-type batteries without the aid of a reducing agent by varying reaction temperature and time (Guimaraes et al., 2022). The PLS is treated by subsequent purification, separation and recovery steps like precipitation, cementation, solvent extraction, and crystallization. The metals are then typically recovered as high purity salts (Mossali et al., 2020, Or et al., 2020, Thompson et al., 2020), while the graphite particles remain undissolved in the acidic media. The H_2SO_4 solution does not significantly change the morphology of the graphite which could be recovered by filtering (Chernyaev et al., 2023, Permathilake et al., 2023). However, there is limited information published so far regarding LTO recycling. Furthermore, the few examples available on this topic have focused on the leaching of Li and Ti from the anode structures, but have neglected the means for separation of LTO from other active materials likely found in the EoL battery streams (Tang et al., 2014; Kumar et al., 2023). Some other studies explored the separation of $\text{Li}_{6.5}\text{La}_3\text{Zr}_{1.5}\text{Ta}_{0.5}\text{O}_{12}$ (LLZTO) electrolyte from an LTO anode and LFP or NMC cathode, either using solutions of HCl (Nowroozi et al., 2022) or citric acid (Waidha et al., 2023). In both cases, TiO_2 was reported as a leach residue due to its high stability.

As mentioned earlier, batteries containing LTO ($\text{Li}_4\text{Ti}_5\text{O}_{12}$) as anode material are slowly gaining popularity in large EV applications. However, graphite remains the most common anode material in LIBs and it is thus likely that, in the future, EoL LIB streams will contain a mixture of LTO and graphite particles along with various cathodic materials.

The present research work explores the potential of froth flotation as an alternative method for graphite recovery from LIB chemistry mixtures containing LTO and NMC chemistries. Flotation is considered a direct recycling method for LIBs, as it preserves the structure of both anode and cathode materials, allowing their recovery for potential remanufacturing of new batteries (Foylan et al., 2021, Rinne et al., 2023, Vanderbruggen et al., 2021a, Verdugo et al., 2022a, Zhan et al., 2018). Preservation of the graphite functional integrity can also improve the recycling economics especially if recovery grades achieve > 99 % (battery grade) purity (Rinne et al., 2023). Furthermore, graphite removal from black mass results in a metal-rich feed, which allows

higher leach throughput volumes that - in turn - can potentially reduce the associated environmental impacts (Vanderbruggen et al., 2021, Zhan et al., 2018).

To the best of the authors' knowledge, graphite recovery from mixed LIB waste containing LTO anodes has not been studied previously using froth flotation. Consequently, it also remains unclear what is the best strategy for the removal of graphite in a hydrometallurgical recycling process. Two potential strategies for the utilization of flotation are presented in Fig. 1, assuming a stream of EoL batteries composed of NMC811 cathode particles mixed with graphite and LTO anode particles. In Recycling Scenario A, froth flotation is studied as a process step prior to hydrometallurgical treatment to remove graphite as a product for direct recycling for new batteries. In this case, the metal containing fraction (Ni, Co, Mn, and Li) would be subjected to hydrometallurgical refining, leaving a residue containing mostly TiO_2 . In Scenario B, the metals (Ni, Co, Mn, and Li) would be first recovered via hydrometallurgical processing, leaving a mixed leach residue of graphite and TiO_2 , which would be then separated by froth flotation. While Scenario A will aid to reduce the material throughput in the leaching unit, this second scenario would prevent inevitable losses of Li and transition metals in the graphite froth stream. Thus, the present work aims to explore the use of flotation as means for the recovery of graphite in NMC and LTO mixtures and identify its preferred position in a recycling process.

2. Materials and experimental procedures

It is worth acknowledging that organic compounds such as the binder, carbon black and electrolyte residue present in spent LIBs can form hydrophobic coatings on the Li-metal-oxide particles thereby reducing their hydrophobic differences *cf.* graphite. Consequently, a significant portion of research on the use of froth flotation as a recycling method for spent LIBs has focused on the effect of different pre-treatments like dissolution, pyrolysis and attrition on the liberation of active particles (Makuza et al., 2021, Qiu et al., 2022, Salces et al., 2022, Vanderbruggen et al., 2022b, Yang et al., 2021, Zhan et al., 2018).

Since this work focuses on the separation differences between the individual active material particles in a mixture of NMC811-LTO-graphite, a synthetic mixture of pure components was used, assuming that prior pre-treatments have resulted in a complete liberation of the particles. Accordingly, the observed behavior can be associated to the fundamental properties of the active materials. Admittedly, this likely represents a deviation from the behavior of real EoL batteries.

2.1. Minerals and reagents

Model black mass samples were prepared by mixing battery grade graphite (PG1110, ProGraphite GmbH, Untergriesbach, Germany), NMC811 (PO5038, MSE Supplies, Tuscon, AZ, USA) and LTO (PO0196, MSE Supplies, Tuscon, AZ, USA) with various mass composition ratios (e.g., 1:1 graphite:NMC811; 1:1 graphite:LTO; 2:1:1 graphite:LTO:NMC811; 2:1:1 NMC811:LTO:graphite). These ratios were chosen to represent the typical mass composition of cathode and anode materials in single-type LIBs, and arbitrarily assuming that EoL streams with mixed chemistries will contain a similar proportion of LTO and graphite-containing batteries. Also, a model leach residue comprised of 50 wt% pure graphite and 50 wt% TiO_2 particles (232033, Merck (Sigma-Aldrich, Finland)) was also used to evaluate Recycling Scenario B outlined in Fig. 1, where froth flotation is used to recover graphite and TiO_2 after the hydrometallurgical extraction of Ni, Co, Mn, and Li. The particle size distributions of the materials used in this study were measured by laser diffraction (Malvern Mastersizer 3000, Malvern, UK) and the results are shown in Fig. 2. Fine TiO_2 powder was used since this is the likely size range of the residue obtained after leaching LTO anode crystals (Tang et al., 2014).

Methyl isobutyl carbinol (MIBC), $((\text{CH}_3)_2\text{CHCH}_2\text{CH}(\text{OH})\text{CH}_3)$ (109916, Merck, (Sigma Aldrich, Finland)) was used as the frother as it

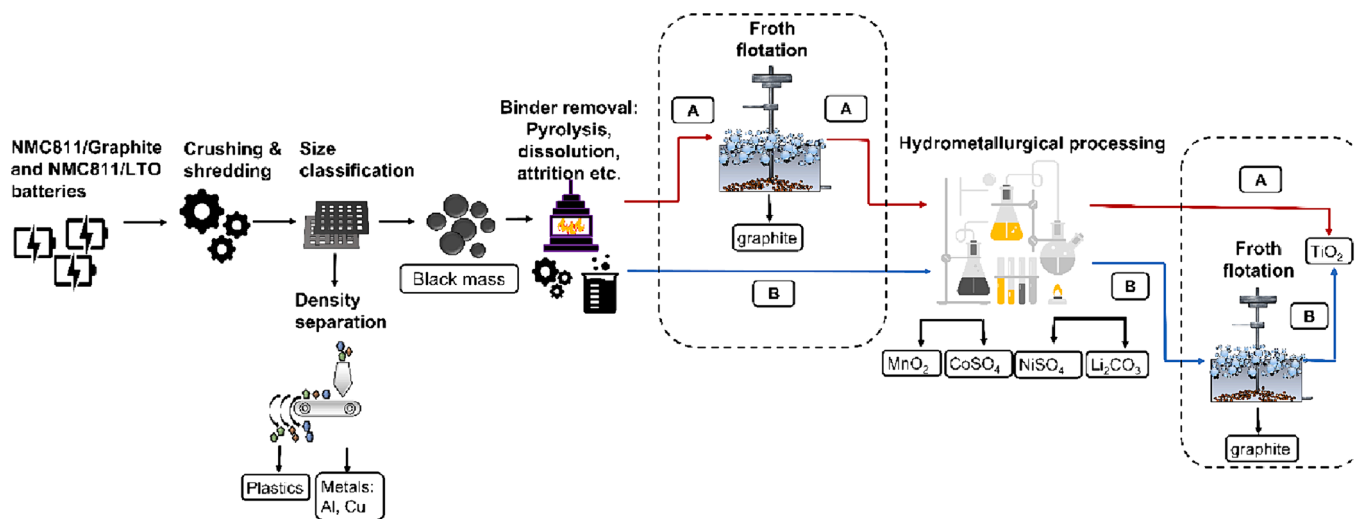


Fig. 1. A potential simplified recycling flow sheet for the NMC811-Graphite-LTO particle mixture, where path A represents a scenario where froth flotation is used to remove graphite before hydrometallurgical material recoveries and path B represents a scenario, where the leach residue is separated using froth flotation. The positions of the two scenarios investigated are highlighted within the flowsheet.

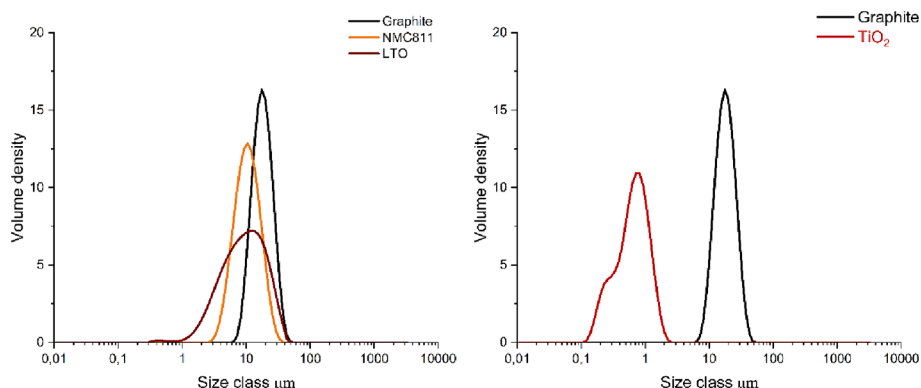


Fig. 2. Particle size distributions of Graphite, NMC811, LTO and TiO₂ powders.

is considered suitable for small particle flotation and has been previously utilized for graphite flotation from black mass (Foylan et al., 2021, Wills et al., 2016). Vanderbruggen et al. (2021a) found that MIBC adsorbs on the surfaces of graphite particles, increasing their hydrophobicity and promoting their attachment to air bubbles, while simultaneously not interacting with the NMC that was also present. Subsequent investigations by Foylan et al. (2021) demonstrated that oily collectors can interact with both NMC and graphite particles, therefore no collector was used in this study.

2.2. Flotation experiments

Flotation experiments were performed using a 1-litre flotation cell (Lab Cell-60 mm FloatForce mechanism, Outotec, Espoo, Finland). In each experiment, 40 g of model black mass was mixed with 1-litre of ultra-high purity water (15 MΩ.cm, purified by Purelab, Elga, High Wycombe, UK). The pulp was mixed in the flotation cell with an impeller speed of 1000 rpm for 3 min. Following the initial agitation, MIBC frother was added to the flotation cell at a concentration of 8 ppm and mixing was continued for another 2 min. The impeller speed was then reduced to 850 rpm and air was fed at a flow of 2 l/min, to initiate the flotation experiment. The experimental parameters are summarized in Table S1.

As the froth rose, it was manually scooped to produce concentrate samples, which were collected at intervals of 0–1 min, 1–3 min and 3–8 min

to study the kinetics of the flotation process. Fig. 3 outlines a schematic of the froth flotation experiments conducted in this study. As previous researchers have found that Li readily dissolved into the process water (Verdugo et al., 2022a), preliminary experiments to determine the mass losses of NMC811 and LTO was carried out. In these measurements, 10 g of NMC811 or LTO were mixed for 8 min in a

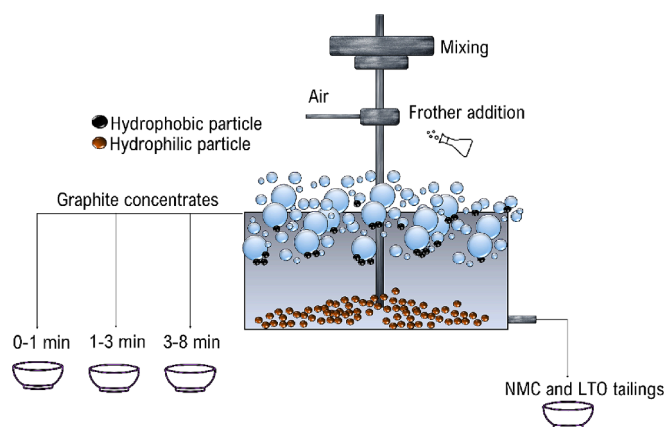


Fig. 3. A schematic representation of the froth flotation apparatus and the experiments.

flotation cell at 850 rpm impeller speed, after which the mass loss was measured.

The collected concentrates and the remaining pulp in the flotation cell were filtered and dried in a convection oven under ambient air at 40 °C for approximately 2 days. The graphite-TiO₂ concentrates were not filtered as the fine TiO₂ particles blocked the filters. Therefore, the collected concentrates and residual pulp were dried by evaporation in a

convection oven at 80 °C.

2.3. Characterization of froth concentrates and the tailings

Dried froth concentrates were weighed, and their chemical compositions were analyzed with a portable handheld X-ray Fluorescence (XRF) device (Oxford Instruments, X-MET 5000, Abingdon, UK). For a

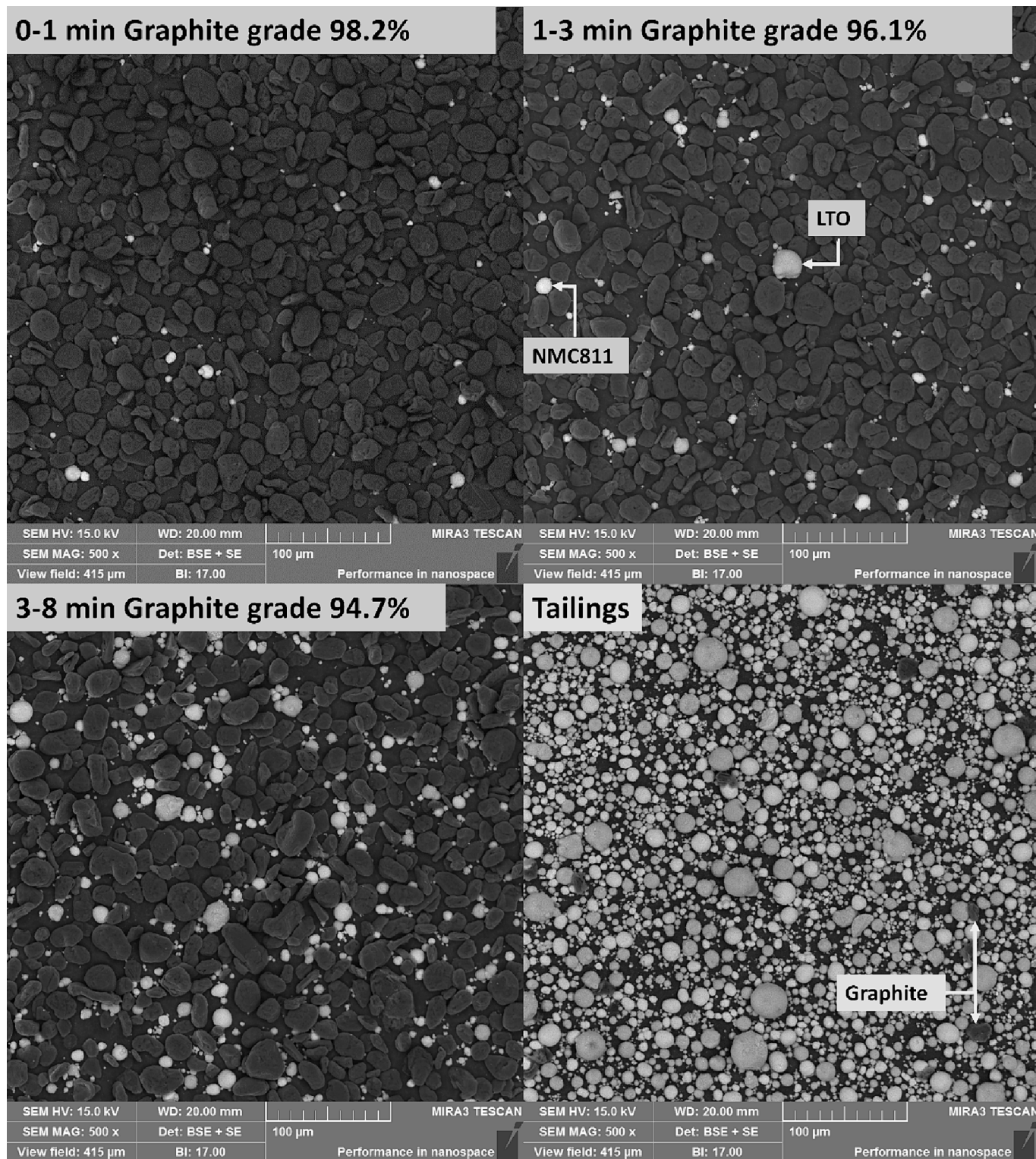


Fig. 4. Graphite concentrates collected from 50 wt% graphite, 25 wt% NMC811 and 25 wt% LTO mixture during 0–1 min, 1–3 min and 3–8 min flotation times. Based on the Energy dispersive spectrometry (EDS) analysis, black particles are graphite, grey particles are LTO, and white particles are NMC811.

reliable quantitative analysis with XRF, calibration curves were constructed using benchmark mixtures of graphite-LTO-NMC811 and graphite-TiO₂ with known composition. As XRF is unable to detect Li or oxygen, Ti and Ni were used as markers for the studied Li-metal-oxides and TiO₂, with each composition reported is an average of five measurements. The calibration data for the XRF is available in the [Supplementary Information \(Figures S1-S3\)](#). Based on the recovered mass and graphite grades of the collected froth concentrates, the cumulative recoveries as a function of time and the cumulative grades were calculated to evaluate flotation performance.

Image analysis with Scanning Electron Microscopy - Energy Dispersive X-ray Spectroscopy (SEM-EDS, MIRA3 SEM, Tescan, Brno, Czech Republic and UltraDry Silicon Drift Energy Dispersive X-Ray Spectrometer) were carried out to characterize the distributions and morphologies of the graphite, LTO, and NMC811 particles in the recovered graphite concentrates and tailings. EDS analyses were taken from each collected graphite concentrate sample—comprised of the powder attached to carbon tape—based on three random surface locations. SEM images were measured using a 15 kV acceleration voltage with signals from the back scattered electron detector and secondary electron detector combined to provide phase composition and particle morphology information. EDS analyses were made using counting time 20 s per spectrum, Phi-Rho-Z type of matrix correction algorithm, and Mineral standards by Astimex Scientific (Toronto, Ontario, Canada).

3. Results and discussion

3.1. Model Graphite-NMC811-LTO system

It is generally accepted that graphite particles are hydrophobic, whereas the immersion of Li-metal-oxides in water results in a hydrated surface layer that is hydrophilic in nature (Vanderbruggen et al., 2021a, [Wills et al., 2016](#), [Zhan et al., 2018](#)). Nonetheless, despite the wettability differences, a portion of the LTO and NMC811 particles get collected along with the graphite particles, whilst some graphite is lost into tailings. SEM images displayed in [Fig. 4](#) show the particle morphologies of the recovered graphite fractions as a function of flotation time. EDS mapping of Ti and Ni is shown in [Figure S4](#).

In flotation, particles are transported to the froth either by entrainment, entrapment, or true flotation mechanisms. Particle recovery by true flotation requires a collision between the particle and the bubble, which results in a stable attachment. Hydrodynamic forces control the probability of collisions between particles and bubbles, while the formation and stability of particle-bubble aggregates depend on the hydrophobicity of particles ([Ata et al., 2002a](#), [Subrahmanyam et al., 1988](#), [Wills et al., 2016](#),). Entrainment, contrary to true flotation, is an unselective mechanism by which particles are transported into the froth. As water is carried into the froth phase, it will bring with it dispersed particles, independent of their hydrophobicity. In this case, the recovery of entrained particles shows a linear correlation with the water recovery ([Ata et al., 2003b](#), [Subrahmanyam et al., 1988](#), [Wills et al., 2016](#), [Zhan et al., 2018](#)). Furthermore, since gravitational pull is weaker on finer particles, it is widely acknowledged that entrainment favors particles with small size.

Several researchers ([Rinne et al., 2023](#), [Vanderbruggen et al., 2021a](#), [Verdugo et al., 2022a](#)) have studied graphite separation from perfectly liberated model black mass samples using froth flotation. [Rinne et al., \(2023\)](#) reportedly improved the graphite grades by reducing the percentage of fine < 10 µm LCO particles in the black mass with a selective flocculation method. Both [Vanderbruggen et al., \(2021a\)](#) and [Verdugo et al., \(2022a\)](#) measured linear correlations between the recovery of NMC111, LCO and NCA and water content in the froth phase, result of which suggested the flotation of cathode materials via entrainment. Interestingly, captive bubble measurements conducted by [Vanderbruggen et al., \(2021a\)](#) showed that Li-metal oxide particles can also attach to air bubbles, particularly in the presence of oily collectors. It is

thus possible that, under certain circumstances, both entrainment and true flotation of lithium metal oxide particles occur simultaneously. As shown in [Fig. 4](#), the presence of the larger NMC and LTO particles in the graphite concentrates increases with time. With longer collection time, the entrainment recovery also increases ([Wills et al., 2016](#)). True flotation of the NMC811 and LTO particles should also increase with time as graphite is removed from the flotation cell, increasing the probability of kinetically less favored interactions between the larger number of available bubbles and lithium metal oxides.

The graphite grade-recovery curves and recovery kinetics from all the tested graphite-NMC811-LTO compositions ([Fig. 5](#)) provide further evidence of the interactions between these particles in the flotation cell - cumulative graphite grades and recoveries of all experiments are provided in [Tables S2-S4](#). Graphite flotation kinetics were determined by fitting the graphite recoveries collected at different time intervals to the classical first order kinetic model according to equation (1) to obtain the rate constant *k* ([Wills et al., 2016](#)).

$$R(t) = R_{max}(1 - e^{-kt}) \quad (1)$$

where, *R*(*t*) is the recovery of graphite at time (*t*) and *R*_{max} is the theoretical maximum recovery.

Comparison of the graphite flotation kinetics from different graphite-LTO-NMC811 compositions indicates that the concentration of graphite or NMC811 within the mixture does not influence the graphite flotation rate. For example, the *k* values are similar, *k* = 0.88 min⁻¹ and 0.87 min⁻¹, for the mixtures containing 50 wt% NMC811, 25 wt% LTO, 25 wt% Graphite and 50 wt% Graphite, 25 wt% LTO, 25 wt% NMC811, respectively. Each datapoint in [Fig. 5](#) represents the average of results from the same repeated experiment. The standard deviations of the kinetic datapoints of graphite flotation measured in the two component mixtures containing only graphite and NMC811 or graphite and LTO are smaller when compared to the three component systems as it may be that adding components increases the random interactions in the flotation cell. Interestingly, the LTO concentration in the mixture has a significant effect on the kinetics of graphite flotation. The lowest graphite flotation kinetics (*k* = 0.68 min⁻¹) is observed in the absence of LTO, whereas 50 wt% of LTO resulted in the highest rate measured (*k* = 1.17 min⁻¹).

The higher froth stability improves the recovery rate of hydrophobic particles as a stable froth promotes a longer particle residence time, which increases the probability of collecting more particles ([Ata et al., 2002a](#)). In contrast, when the bubbles in the froth layer begin to pack together, the water film between them is squeezed and drains out, resulting in bubble coalescence that leads to froth collapse. Froth stability in a simple gas-liquid system depends on the stability of the liquid film separating the bubbles. In mineralized froths, the hydrophobic particles—in this case graphite—can stabilize the froth by attaching to the air-water interface thus preventing bubble coalescence upon collision. Additionally, the presence of hydrophilic particles in the froth has been observed to decrease the bubble coalescence rate, which is hypothesized to be the result of increased viscosity of the water particle suspension retained in the water film between the bubbles. Consequently, this higher viscosity reduces drainage rate of the water film reducing the coalescence rate of the bubbles. ([Ata et al., 2003b](#)).

The distributions of LTO and NMC811 impurity particles in the graphite concentrates were analyzed with EDS and XRF measurements. Only a fraction of the identified particles could be analyzed by EDS, which means that this method has an intrinsic statistical inaccuracy. Nevertheless, [Fig. 6](#) shows that the LTO particles are always found in the graphite concentrates in larger quantities compared to the NMC811 particles.

Despite their similar particle size distributions, the LTO particles are more likely to be entrained in the froth in higher quantities than NMC811 particles due to their lower density: LTO = 3.5 g/cm³ *cf.* NMC811 = 4.8 g/cm³. This also means that more of the LTO particles

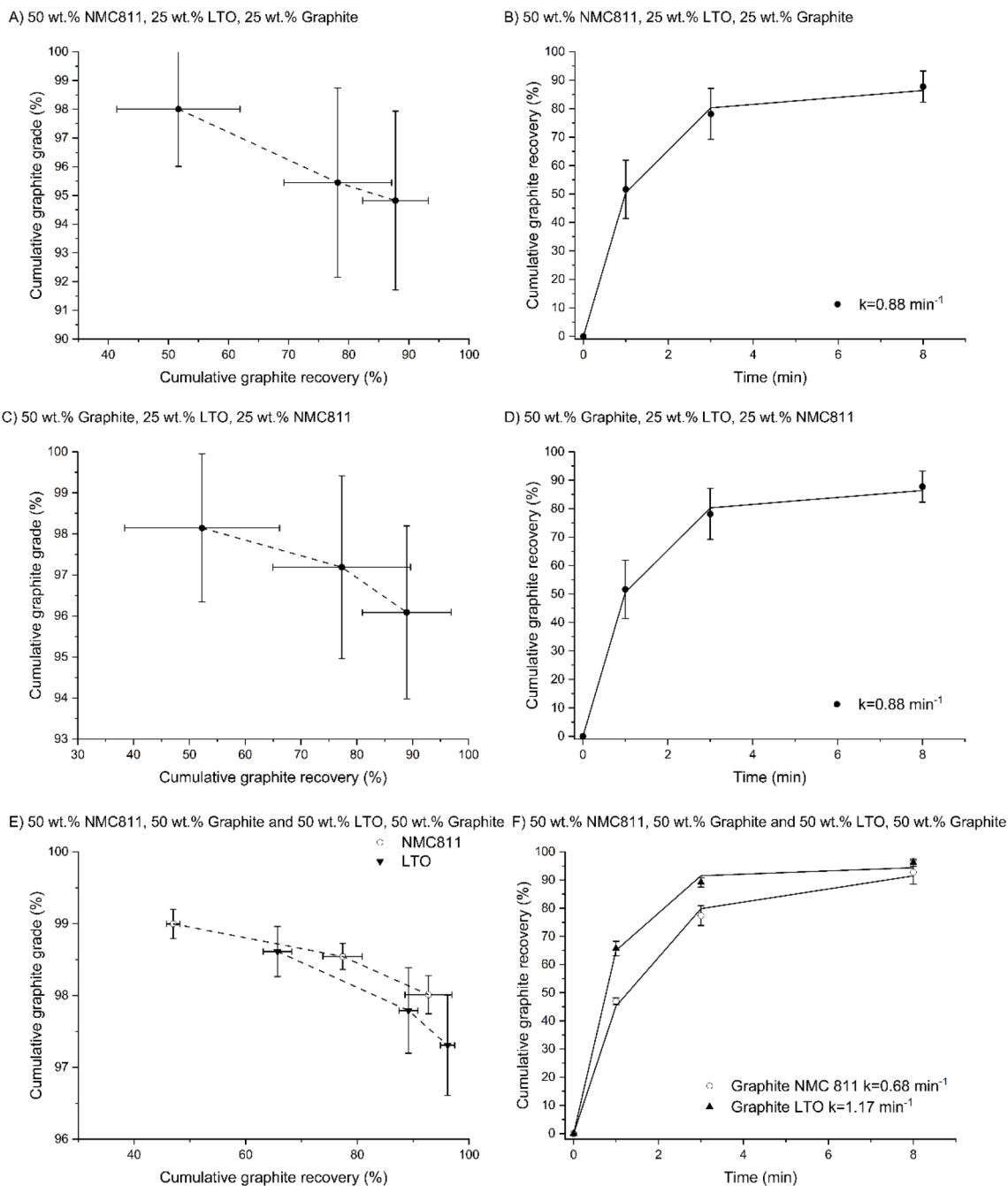


Fig. 5. Relationship between graphite recovery and grade and graphite flotation kinetics in a 40 g/l solid liquid ratio suspension containing different ratios of graphite, LTO and NMC811 particles. The datapoints presented are averages of repeated experiments (4–7 repetitions per datapoint) and the standard deviation is shown as the experimental error of each experiment.

would be present in an equal mass of sample compared to NMC811 particles.

Therefore, the increase in graphite recovery kinetics as a function of higher LTO concentration in the flotation cell, could be explained by a larger quantity of entrained LTO particles in the froth. These entrained LTO particles would increase the liquid film viscosity between the bubbles, thereby reducing water drainage and bubble coalescence. This improved froth stability would lead to longer particle residence time in the froth and result in a higher collection rate of the graphite and the entrained particles increasing the measured kinetics of graphite recovery, while conversely reducing the graphite grade *cf.* graphite-NMC811 system.

As stated by [Ata et al., \(2003\)](#), the viscosity of a suspension can be defined using Equation (2), following the correlation established in the seminal work by [Chung et al., \(1978\)](#):

$$\mu^* = \mu \left(1 + 2.5 \left(\frac{X_s}{X_s + \frac{\rho_s}{\rho}} \right) + 4.375 \left(\frac{X_s}{X_s + \frac{\rho_s}{\rho}} \right)^2 \right) \quad (2)$$

where μ^* is the viscosity of the suspension, μ is the viscosity of water, X_s is the solid concentration in the suspension, ρ is the density of the liquid and ρ_s is the density of the solid.

Equation (2) indicates that lower density particles increase the viscosity of the suspension more than higher density particles. It is

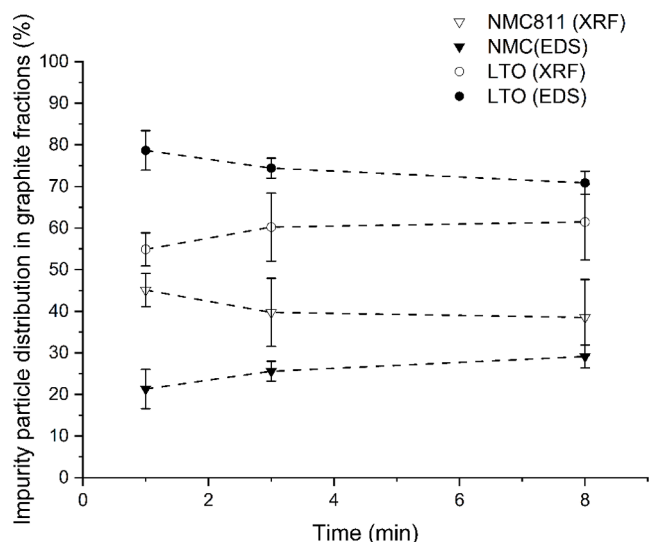
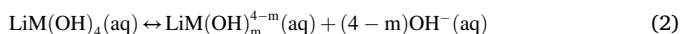


Fig. 6. Distribution between LTO particles and NMC811 particles in the recovered graphite concentrates during flotation of 50 % graphite, 25 % NMC811, 25 % LTO mixture.

therefore possible that the increased viscosity of the water film between the bubbles, in addition to the increased entrainment effect of the LTO particles, is further attributed to their lower density compared to the NMC811 particles.

Other theories on froth stability can also be found in the literature. Destabilizing effects of the fine ($<30\ \mu\text{m}$) particles have been attributed to MIBC adsorption on the particle surfaces. This reduces the MIBC concentration in the flotation cell, producing weaker froth (Wills et al., 2016), however, this may not be a likely explanation for the differences in the graphite recovery kinetics, since MIBC has been observed to adsorb on the graphite particle surfaces by Vanderbruggen et al. (2021a). Nonetheless, the different graphite concentrations investigated in this research do not appear to influence the graphite recovery kinetics. MIBC adsorption onto the NMC811 particle surfaces could explain the weaker froth and reduced graphite recovery rates compared to high graphite flotation rates in the presence of LTO, although a difference in the NMC811 concentration does not seem to influence the graphite recovery kinetics. In addition, Vanderbruggen et al. (2021a) concluded that MIBC does not interact with the NMC111 particles.

The NMC811-LTO-graphite mixture was observed to generate a highly alkaline solution with pH values close to 11. This is explained by the leaching of lithium into the process water and forming hydroxyl ions according to reactions (1) - (2) (Verdugo et al., 2022a).



where M is the metal cation in the oxide and m is the number of molecules involved during the reaction.

Verdugo et al. (2022a, 2023b) observed a correlation between graphite recovery kinetics and Li^+ concentration in the flotation cell with the fastest graphite recovery achieved at the highest Li^+ concentration. Conversely, a high lithium concentration simultaneously increases the recovery of lithium metal oxides by entrainment, reducing the quality of the recovered graphite. Dissolved Li^+ ions, due to their small radius, can readily interact with water molecules and polarize them, which strengthens the electrostatic bonds between the water molecules (Salces., 2022). Dissolved ions stabilize froths by reducing water drainage of the liquid film between the bubbles (Verdugo et al., 2023b).

Despite the LTO and NMC811 impurity particles found in the

collected graphite concentrates, high grade graphite product ($>98\%$ purity) could be recovered in most experiments. However, the recovery percentage of the high purity graphite depends on the lithium metal oxide particle mixture, from which the graphite is collected. This result demonstrates that froth flotation has the potential to be used as direct recycling method to produce anode raw material for new batteries, if the process parameters such as solid concentration, particle size, air flow rate, collector and depressant chemicals and dosages etc. are optimized and a high degree of liberation of active material particles during the pre-treatments is achieved.

3.2. Model Graphite-TiO₂ leach residue

The applicability of froth flotation as a potential solution for treating leach residues containing graphite and TiO₂ was studied by composing a model leach residue consisting of perfectly liberated TiO₂ and graphite particles, assuming that all Li has been recovered as Li₂CO₃ or LiOH if prior hydrometallurgical recovery processes would have been applied. This would potentially leave only graphite and TiO₂ in the leach residue from the LTO particles. The SEM images presented in Fig. 7 show the increasing presence of TiO₂ in the concentrate samples as the flotation experiment progressed. Very fine TiO₂ particles have a tendency of clustering together after the graphite has been collected, and therefore the powder samples were observed to have a non-uniform consistency (see Fig. 7).

The grade-recovery curves and recovery kinetics for graphite flotation from a mixture containing 50 wt% graphite and 50 wt% TiO₂ particles are displayed in Fig. 8 and associated numerical values can be found in Table S5. Results show that the graphite recoveries are significantly higher, and the flotation kinetics considerably faster ($k = 1.84\ \text{min}^{-1}$) compared to the graphite recoveries obtained from the graphite-NMC811-LTO system. Nonetheless, this faster and higher graphite recovery has a reduced grade when compared to graphite recoveries from the graphite-NMC811-LTO system.

The fastest graphite recovery kinetics and the lowest grades from all the studied suspensions show that the very fine TiO₂ particles are heavily entrained in the froth. It could be assumed that the hydrophilic TiO₂ particles (Wills et al., 2016), due to their lightness and small size, are suspended in large quantities within the water film surrounding the bubbles and therefore result in the largest increase in the water film viscosity of all the graphite-oxide systems of this study. Fig. 9 illustrates that the very fine TiO₂ particles have a tendency to form coatings on graphite particle surfaces, which in addition to significantly lowering the graphite grade, such TiO₂ coated graphite particles may not be easily usable for the direct recycling of graphite as new battery anodes. Therefore, it is recommended to apply froth flotation prior to the hydrometallurgical processes to ensure maximum recovery of high-grade graphite.

4. Conclusions

In this experimental research, perfectly liberated synthetic graphite-NMC811-LTO black mass samples and synthetic graphite-TiO₂ leach residue were separated by froth flotation. Approximately 52 – 54 % of the graphite could be recovered with high grade ($>98\%$ purity) from the model black mass before hydrometallurgical recycling. Using froth flotation to separate leach residue containing TiO₂ and graphite particles may not be as optimal as incorporating froth flotation step before the hydrometallurgical recycling processes. High graphite recovery kinetics was obtained in the presence of ultrafine TiO₂ particles, but the graphite grades were the lowest of all experiments conducted in this study, on average $<96\%$. In addition, ultrafine TiO₂ particles have a tendency of coating the graphite particles, which might make its use in new battery cells challenging.

LTO particles were observed to contaminate the graphite fractions more than the NMC811 particles. This can be explained by stronger

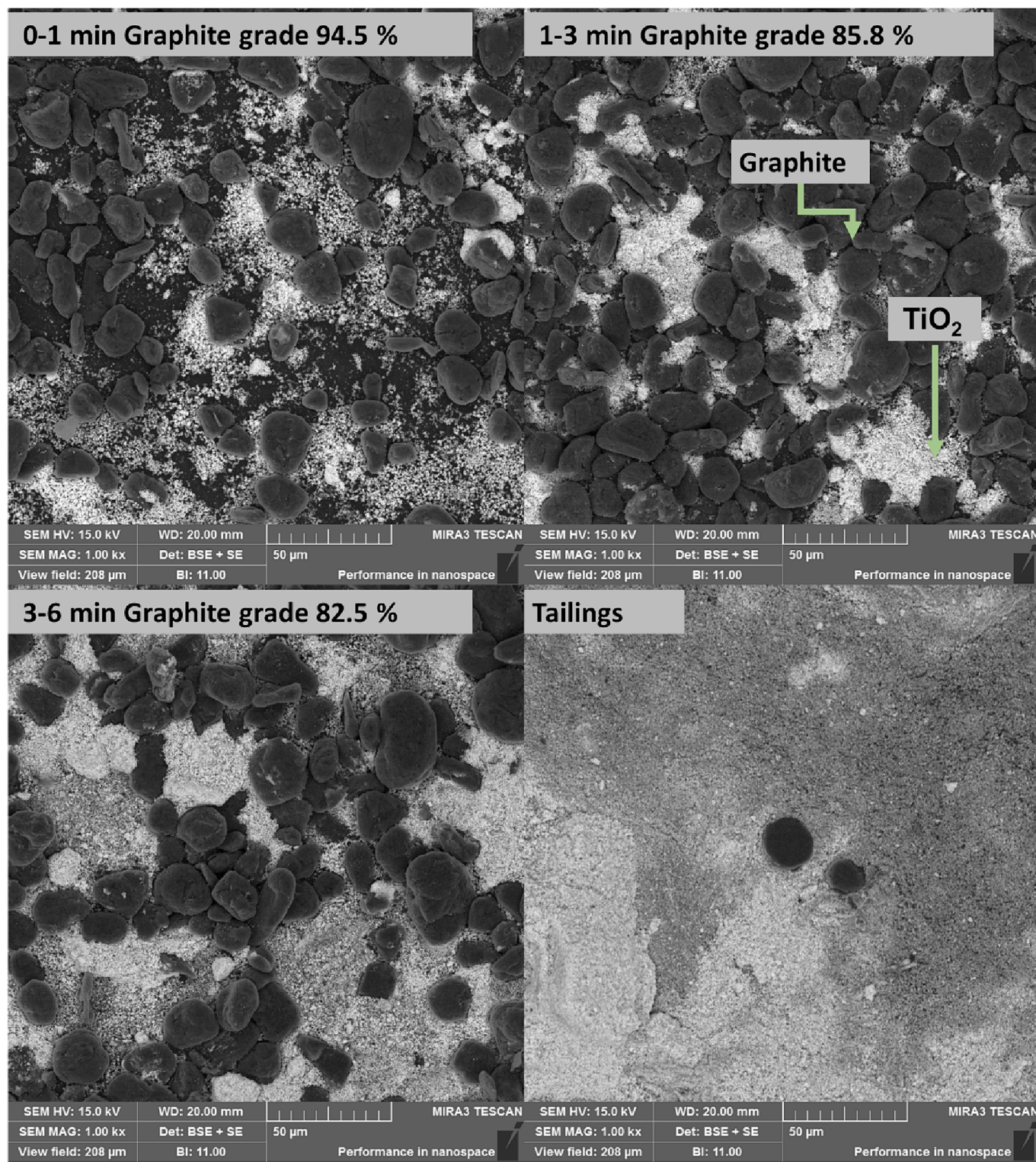


Fig. 7. Graphite concentrates collected from 50 wt% graphite, 50 wt% TiO₂ mixture during 0–1 min, 1–3 min and 3–6 min flotation times. Black particles are graphite and white particles are TiO₂.

entrainment of the LTO particles to the froth because of their larger quantity and lower density compared to the heavier NMC811 particles. Even though the grades of the recovered graphite concentrates were similar, the kinetics of graphite flotation had measurable differences depending on the LTO concentration in the suspension. Increasing LTO concentration was observed to increase the recovery kinetics of graphite, whereas differences in the NMC811 or graphite concentration

did not have a similar effect. It is possible that the entrained LTO particles increase the viscosity of the water film between the bubbles more compared to the entrained NMC811 particles because of their lower density thus slowing the bubble coalescence time and thereby increasing the stability of the froth. A more stable froth allows longer residence time for the particles in the froth phase, which increases their collection probability. Therefore, the percentage of the recovered high-grade

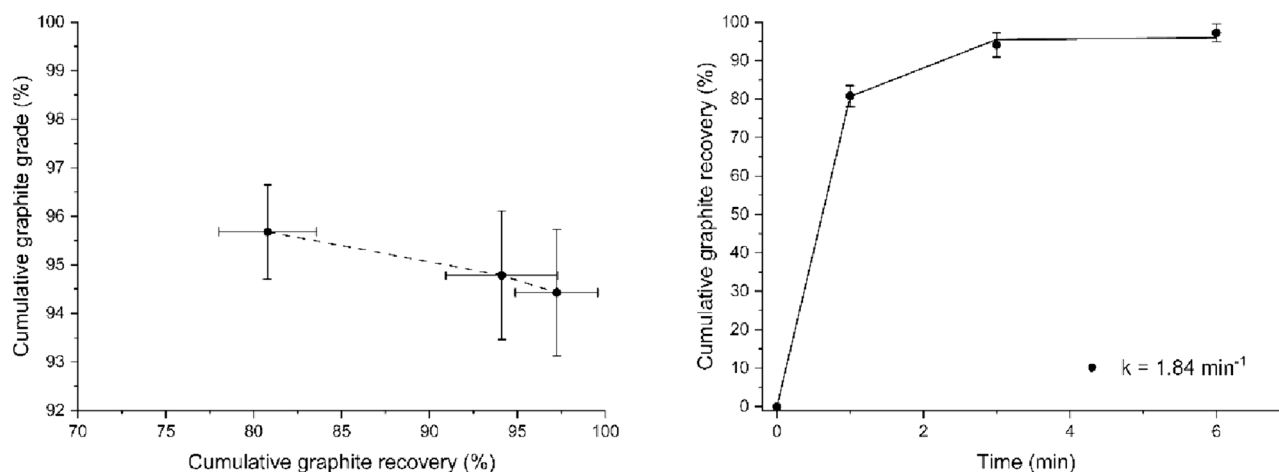


Fig. 8. Relationship between graphite recovery and grade and graphite flotation kinetics in 40 g/l solid liquid ratio suspension containing 50 wt% graphite and 50 wt % TiO_2 particles. The datapoints presented are averages of 4 repeated experiments and standard deviation is shown as the experimental error of each experiment.

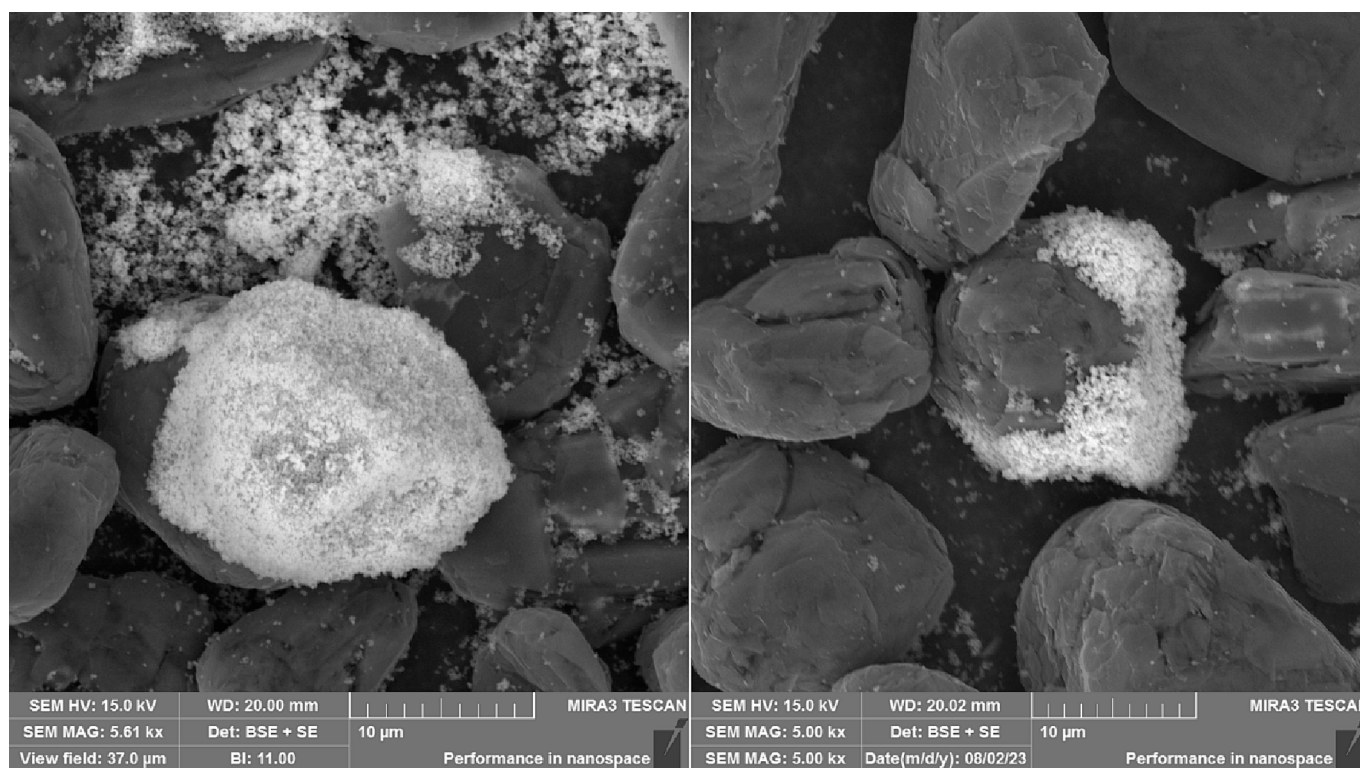


Fig. 9. TiO_2 particles forming coatings on graphite particles during froth flotation.

graphite varies depending on the composition of the particle mixture in the flotation cell.

This research demonstrates that if the pre-treatment processes can achieve high degree of separation and operational parameters such as air flow rates, mixing speeds and solid–liquid ratios are well optimized, froth flotation has the potential to be used as a direct recycling method to produce battery grade graphite for new battery cells. It is recommended to continue the research in the future by including the effect of modifying the surface charges of the LIB particles by pH adjustment. This would improve the particle separation efficiencies by allowing optimal selections of flotation reagents such as flocculants, ionic collectors and depressants.

CRediT authorship contribution statement

Hanna Sahivirta: Conceptualization, Investigation, Writing – original draft, Methodology. **Benjamin P. Wilson:** Conceptualization, Data curation, Writing – review & editing. **Mari Lundström:** Funding acquisition, Writing – review & editing. **Rodrigo Serna-Guerrero:** Formal analysis, Funding acquisition, Supervision, Writing – review & editing.

Declaration of competing interest

The authors declare that they have no known competing financial interests or personal relationships that could have appeared to influence the work reported in this paper.

Data availability

Data will be made available on request.

Acknowledgments

This research has been funded by the HELIOS project, supported by the European Union's Horizon 2020 research and innovation programme under grant agreement No. 963646. The authors would also like to thank Lotta Nenonen for conducting some flotation experiments. In addition, the authors would like to acknowledge the use of the facilities provided by the Academy of Finland's RawMatTERS Infrastructure (RAMI-FIRI) based at Aalto University.

Appendix A. Supplementary data

Supplementary data to this article can be found online at <https://doi.org/10.1016/j.wasman.2024.03.032>.

References

- Ata, S., Nafis, A., Jameson, G.J., 2002. Collection of hydrophobic particles in the froth phase. *Int. J. Miner. Process.* 64, 101–122. [https://doi.org/10.1016/S0301-7516\(01\)00066-7](https://doi.org/10.1016/S0301-7516(01)00066-7).
- Ata, S., Nafis, A., Jameson, G.J., 2003. A study of bubble coalescence in flotation froths. *Int. J. Miner. Process.* 72, 255–266. [https://doi.org/10.1016/S0301-7516\(03\)00103-0](https://doi.org/10.1016/S0301-7516(03)00103-0).
- Casals, L.C., García, B.A., Aguesse, F., Iturrondobetia, A., 2017. Second life of electric vehicle batteries: relation between materials degradation and environmental impact. *Int. J. Life Cycle Assess.* 22, 82–93. <https://doi.org/10.1007/s11367-015-0918-3>.
- Changes, A., Swiatowska, J., 2015. *Lithium Process Chemistry: Resources, Extraction, Batteries and Recycling*. Elsevier Amsterdam, Lithium Battery Technologies: From the Electrodes to the Batteries, 125–154.
- Chernyaev, A., Kobets, A., Liivand, K., Tesfaye, F., Hannula, P., Kallio, T., Hupa, L., Lundström, M., 2023. Graphite recovery from waste li-ion battery black mass for direct re-use. *Miner. Eng.* 208, 108587 <https://doi.org/10.1016/j.mineng.2024.108587>.
- Chung, Y.M., Adelman, S.A., 1978. Transport properties of concentrated polymer solutions. hydrodynamic mean field theory of the viscosity of a sphere suspension. *J. Chem. Phys.* 69, 3146–3149. <http://pascalfrancis.inist.fr/vibad/index.php?action=getRecordDetail&idt=PASCAL7960177129>.
- Costa, C.M., Barbosa, J.C., Concalves, R., Castro, H., Del Campo, F.J., Lanceros-Mendez, S., 2021. Recycling and environmental issues of lithium-ion batteries: advances. Challenges and Opportunities, *Energy Storage Mater.* 37, 433–465. <https://doi.org/10.1016/j.ensm.2021.02.032>.
- Doose, S., Mayer, J.K., Michalowski, P., Kwade, A., 2021. Challenges in ecofriendly battery recycling and closed material cycles: a perspective on future lithium battery generations. *Metals* 11, 291. <https://doi.org/10.3390/met11020291>.
- European Commission, Directorate-General for Internal Market, Industry, Entrepreneurship and SMEs, Grohol, M., Veeh, C., Study on the critical raw materials for the EU 2023 – Final report, Publications Office of the European Union, 2023, <https://data.europa.eu/doi/10.2873/725585>.
- European Commission, 2020. *Communication from the Commission to the European Parliament, the Council, the European Economic and Social Committee and the Committee of the Regions, Critical Raw Materials resilience: Charting a Path towards greater Security and Sustainability*, Brussels, 3.9.2020. COM 474, final.
- Gaines, L., Richa, K., Spangenberg, J., 2019. Key issues for li-ion battery recycling. *MRS Energy Sustain.* 5, 1–14. <https://doi.org/10.1557/mre.2018.13>.
- Guimaraes, L.F., Botelho Junior, A.B., Espinosa, D.C.R., 2022. Sulfuric acid leaching of metals from waste li-ion batteries without using reducing agent. *Miner. Eng.* 183, 107597 <https://doi.org/10.1016/j.mineng.2022.107597>.
- Integrity exports, 2011, Mitsubishi Chooses Super-Efficient Toshiba SCiB Battery For EVs, <https://integrityexports.com/blog/mitsubishi-chooses-toshiba-scib-battery-for-evs/>.
- Jena, K.K., AlFantazi, A., Ahmad, T.M., 2021. Comprehensive review on concept and recycling evolution of lithium-ion batteries (LIBs). *Energy Fuels* 35, 18257–18284. <https://doi.org/10.1021/acs.energyfuels.1c02489>.
- Kane, M., 2020, InsideEVs, A Journey Into History: 2006 Electric Phoenix Pickup Truck With 35 kWh Battery. <https://insideevs.com/features/414750/history-2006-electric-phoenix-pickup-truck/>.
- Kim, S., Bang, J., Yoo, J., Shin, Y., Bae, J., Jeong, J., Kim, K., Dong, P., Kwon, K., 2021. A comprehensive review on the pretreatment process in lithium-ion battery recycling. *J. Clean. Prod.* 294, 126329 <https://doi.org/10.1016/j.jclepro.2021.126329>.
- Kingsley, N., 2019-10-30. Earthquake mode' battery packs to be fitted to N700S Shinkansen fleet. *Railway Gazette International*. Retrieved 2019-12-04. <https://www.railwaygazette.com/high-speed/earthquake-mode-battery-packs-to-be-fitted-to-n700s-shinkansen-fleet/54936.article>.
- Kumar, B., Srivastava, R.R., Barik, S.P., 2023. Hydrometallurgical recycling of lithium-titanate anode batteries: leaching kinetics and mechanisms, and life cycle impact assessment. *Miner. Eng.* 202, 108289 <https://doi.org/10.1016/j.mineng.2023.108289>.
- Makuza, B., Tian, Q., Guo, X., Chattopadhyay, K., Yu, D., 2021. Pyrometallurgical options for recycling spent lithium-ion batteries: a comprehensive review. *J. Power Sources* 491, 229622. <https://doi.org/10.1016/j.jpowsour.2021.229622>.
- Mossali, E., Picone, N., Gentilini, L., Rodriguez, O., Perez, J.M., Colledani, M., 2020. Lithium-ion batteries towards circular economy: a literature review of opportunities and issues of recycling treatments. *J. Environ. Manage.* 264, 110500 <https://doi.org/10.1016/j.jenvman.2020.110500>.
- Nowroozi, M.A., Waidha, A.I., Jacob, M., van Aken, P.A., Predel, F., Ensinger, W., Clemens, O., 2022. Towards recycling of LLZO solid electrolyte Exemplarily performed on LFP/LLZO/LTO cells. *ChemistryOpen* 11, e202100274.
- Or, T., Gourley, S.W.D., Kaliyappan, K., Yu, A., Chen, Z., 2020. Recycling of mixed cathode lithium-ion batteries for electric vehicles: current status and future outlook. *Carbon Energy* 2, 6–43. <https://doi.org/10.1002/cey2.29>.
- Page, L., 2008, Blighty's electro-supercar 2.0 unlocked today, https://www.theregister.com/2008/07/22/lightning_fast_charge_supercar/.
- Pagliaro, M., Meneguzzo, F., 2019. Lithium battery reusing and recycling: a circular economy insight. *Heliyon* 5, e01866.
- Permathilake, D.S., Botelho Junior, A.B., Colombi, F., Tenorio, J., Espinosa, D., Vaccari, M., 2023. Valorization of waste graphite deriving from "End of Life Lithium-Ion Battery recycling" for a second use in wastewater treatment. 18th International Conference on Environmental Science and Technology, Athens, Greece. DOI: 10.30955/gnc2023.00266.
- Proterra, <https://www.proterra.com/>.
- Qiu, H., Peschel, C., Winter, M., Nowak, S., Köthe, J., Goldmann, D., 2022. Recovery of graphite and cathode active materials from spent lithium-ion batteries by applying two pretreatment methods and flotation combined with a rapid analysis technique. *Metals* 12, 677. <https://doi.org/10.3390/met12040677>.
- Rinne, T., Araya-Gómez, N., Serna-Guerrero, R., 2023. A study on the effect of Particle size on li ion battery recycling via flotation and perspectives on selective flocculation. *Batteries* 9, 68. <https://doi.org/10.3390/batteries9020068>.
- Salces, A.M., Bremerstein, I., Rudolph, M., Vanderbruggen, A., 2022. Joint recovery of graphite and lithium metal oxides from spent lithium-ion batteries using froth flotation and investigation on process water re-use. *Miner. Eng.* 184, 107670 <https://doi.org/10.1016/j.mineng.2022.107670>.
- Subrahmanyam, T.V., Forssberg, E., 1988. Froth stability, particle entrainment and drainage in flotation — a review. *Int. J. Miner. Process.* 23 (1), 33–53. [https://doi.org/10.1016/0301-7516\(88\)90004-X](https://doi.org/10.1016/0301-7516(88)90004-X).
- Tang, W., Chen, X., Zhou, T., Duan, H., Chen, Y., Wang, J., 2014. Recovery of ti and li from spent lithium titanate cathodes by a hydrometallurgical process. *Hydrometall.* 147–148, 210–216. <https://doi.org/10.1016/j.hydromet.2014.05.013>.
- Thompson, D.L., Hartley, J.M., Lambert, S.M., Shiref, M., Harper, G.D.J., Kendrick, E., Andersson, P., Ryder, K.S., Gaines, L., Abbott, A.P., 2020. The importance of design in lithium-ion battery recycling – a critical review. *Green Chem.* 22, 7585–7603. <https://doi.org/10.1039/D0GC02745F>.
- Vanderbruggen, A., Sygusch, J., Rudolph, M., Serna-Guerrero, R., 2021. A contribution to understanding the flotation behavior of lithium metal oxides and spheroidized graphite for lithium-ion battery recycling. *Colloids Surf. a: Physicochemical and Engineering Aspects* 626, 127111. <https://doi.org/10.1016/j.colsurfa.2021.127111>.
- Vanderbruggen, A., Hayagan, N., Bachmann, K., Ferreira, A., Werner, D., Horn, D., Peuker, U., Serna-Guerrero, R., Rudolph, M., 2022. Lithium-ion battery recycling - influence of recycling processes on component liberation and flotation Separation efficiency. *ACS EST Eng.* 2, 2130–2141. <https://doi.org/10.1021/acsestengg.2c00177>.
- Velazquez-Martinez, O., Valio, J., Santasalo-Aarnio, A., Reuter, M., Serna-Guerrero, R., 2019. A critical review of lithium-ion battery recycling processes from Circular economy perspective. *Batteries* 5, 1–33. <https://doi.org/10.3390/batteries5040068>.
- Verdugo, L., Zhang, L., Saito, K., Bruckard, W., Menacho, J., Hoadley, A., 2022. Flotation behaviour of the most common electrode materials in lithium-ion batteries. *Sep. Purif.* 301, 121885 <https://doi.org/10.1016/j.seppur.2022.121885>.
- Verdugo, L., Zhang, L., Etschmann, B., Bruckard, W., Menacho, J., Hoadley, A., 2023. Effect of lithium ion on the separation of electrode materials in spent lithium ion batteries using froth flotation. *Sep. Purif.* 311, 12324. <https://doi.org/10.1016/j.seppur.2023.123241>.
- Waidha, A.I., Salihovicb, A., Jacobb, M., Vanitab, V., Aktekin, B., Brixid, K., Wissela, K., Kautenburger, R., Janek, J., Ensinger, W., Clemens, O., 2023. Recycling of all-solid-state li-ion batteries: a case study of the Separation of individual components within a system composed of LTO, LLZO, and NMC *ChemSusChem* 16, e202202361.
- Wang, Q., Mao, B., Stoliarov, S.I., Sun, J., 2019. A review of lithium ion battery failure mechanisms and fire prevention strategies. *Prog. Energy Combust.* 73, 95–131. <https://doi.org/10.1016/j.pecs.2019.03.002>.
- Wills, B.A., 2016. *Will's mineral processing technology, an introduction to the Practical aspects of ore treatment and mineral recovery, chapter 12 froth flotation, 8th edition*, Butterworth-Heinemann, pp. 265–368.
- Yang, X., Torppa, A., Kärenlampi, K., 2021. Evaluation of graphite and metals Separation by flotation in recycling of li-ion batteries. *Mater. Proc.* 5, 30. <https://doi.org/10.3390/materproc2021005030>.
- Zhan, R., Oldenburg, Z., Pan, L., 2018. Recovery of active cathode materials from lithium-ion batteries using froth flotation. *Sustain. Mater. Technol.* 17, e00062.